Journal of Food Engineering 345 (2023) 111411

Contents lists available at ScienceDirect

Journal of Food Engineering

journal homepage: www.elsevier.com/locate/jfoodeng

The development and properties of nanoemulsions stabilized with glycated soybean protein for carrying β-carotene

Guanhao Bu [a,*], Chenyu Zhao [a], Meiyue Wang [a], Zhen Yu [a], Hongshun Yang [b], Tingwei Zhu [a]

[a] College of Food Science and Engineering, Henan University of Technology, Zhengzhou, 450001, China
[b] Department of Food Science & Technology, National University of Singapore, Science Drive 2, 117542, Singapore

ARTICLE INFO

Keywords:
Soybean protein isolate
Glycation
Nanoemulsion
Storage stability
Bioaccessibility

ABSTRACT

Plant protein nanoemulsion delivery system has high biocompatibility, but its instability in special environment needs to be solved urgently. In this study, glycated soybean protein isolate (GSPI) was used to the construction of nanoemulsions for carrying β-carotene. The interface properties of GSPI, the stability and digestive properties of nanoemulsions stabilized by GSPI were investigated. The results showed that the diffusion rate of GSPI at oil-water interface decreased, while the permeation and rearrangement rates increased. Moreover, the interfacial film formed by GSPI had higher viscoelasticity. The average particle size of GSPI nanoemulsions was less than 500 nm, and the retention rate of β-carotene was more than 80% during the storage of 28 days. Meanwhile, the bioaccessibility of β-carotene in GSPI nanoemulsions increased to above 70% after in vitro digestion. It is concluded that glycated soybean protein nanoemulsions have good storage stability and can be used to encapsulate and deliver of β-carotene.

1. Introduction

β-Carotene is a typical fat-soluble nutrient, which exists widely in animals and plants (Haskell, 2012). It has important biological functions, such as antioxidant activity and reducing cardiovascular disease risk, skin disease, cancer and eye diseases (Boon et al., 2010). However, β-carotene is insoluble in water and has low oxidative stability and bioavailability, which greatly limits its application in food industry (Donhowe and Kong, 2014). In recent years, some studies have demonstrated that the nanocarrier system using biological macromolecules can improve the water-solubility of fat-soluble nutrients and control their release in gastrointestinal tract (Chen et al., 2014; Kong et al., 2018). Therefore, the bioavailability of fat-soluble nutrients is greatly improved (Afonso et al., 2020; Ma et al., 2022).

Nanoemulsions have the advantages of low cost and high safety because of its simple preparation method and less surfactant (Borba et al., 2019). In addition, nanoemulsions have high kinetic stability and excellent bioaccessibility in gastrointestinal digestion, and show a high application prospect in fat-soluble nutrient delivery system (Chen et al., 2020). Soy protein isolate (SPI) has hydrophobic and hydrophilic groups, which can form an interfacial film at oil-water interface, thus acting as a surfactant. Meanwhile, SPI, as a kind of natural biological macromolecular emulsifier, has the advantages of high stability, bioaccessibility and cell permeability in nanoemulsion delivery system (Bhushani et al., 2016; Tian et al., 2021). In order to further improve the stability of protein-based nanoemulsions in extreme environments such as strong acid and high temperature, proteins are usually treated by different modifications. It was found that protein-polysaccharide complex by glycation had great potential application in the delivery system of nanoemulsions (Semenova, 2017; Wang et al., 2020a).

Glycation is a protein modification method by introducing sugar molecules into polypetide chains, and can improve the solubility, thermal stability and emulsification of protein (Corredig et al., 2011; Peng et al., 2018; Seo et al., 2013; Zhong et al., 2021). Meanwhile, the presence of sugar molecules can slow down the digestion of interfacial proteins and improve the digestion of lipids in the emulsion system, which facilitate the absorption of lipid-soluble bioactive substances (Lesmes and McClements, 2012; Zhong et al., 2019). As an interfacial dispersion system, the formation and stability of emulsion, encapsulation and release of fat-soluble bioactive substances are closely related to the interfacial characteristics of emulsifier. Many studies focused on the improvement of functional properties of soybean protein by glycation modification (Boostani et al., 2017; Caballero and Davidov-Pardo, 2021). However, the effects of glycation on the interface properties of

* Corresponding author.
E-mail address: buguanhao2008@126.com (G. Bu).

https://doi.org/10.1016/j.jfoodeng.2023.111411
Received 19 July 2022; Received in revised form 30 December 2022; Accepted 5 January 2023
Available online 6 January 2023

SPI are still unclear, and the delivery system of glycated soybean protein nanoemulsions is not systematically studied.

The objective of this study is to prepare glycated soybean protein with good interface properties and to construct the nanoemulsions delivery system for carrying β-carotene by glycated soybean protein as emulsifier. In addition, the effects of glycation on storage stability and in vitro digestion properties of nanoemulsions were also investigated. This study will provide theoretical basis for the application of glycated soybean protein in nanoemulsion delivery system of β-carotene.

2. Materials and methods

2.1. Materials

Soybean protein isolate (SPI) was obtained from Henan Kunhua Biotechnology Co., Ltd. (Anyang, China). Glucose (Glu), lactose (Lac), galactose oligosaccharide (GOS) and dextran (Dex) were purchased from Shanghai Yuanye Biotechnology Co., Ltd. (Shanghai, China). Soybean oil was obtained from Yihai Kerry Arawana Holdings Co., Ltd. (Shanghai, China). Deionized water was used for the experiment. Other reagents were purchased from Tianjin Kemiou Chemical Reagent Co., Ltd. (Tianjin, China). All the other chemicals were of analytical reagent grade.

2.2. Preparation of glycated SPI by wet-heating reaction

The mixture of SPI (4%, w/v) in borax-sodium hydroxide buffer (0.05 mol/L, pH 10.0) was stirred for overnight until SPI was dispersed uniformly. Then the solution was kept stirring for another 0.5 h after addition of different reducing sugars (4%, w/v). The mixed suspension was heated in water bath at 80 °C for 210 min (Glu, Lac, GOS) or 360 min (Dex). Afterwards, the reaction was terminated immediately with ice bath. Then the dialysis was performed with deionized water at 4 °C for 48 h. Glycated soybean protein was obtained after dialysis solution was lyophilized. All the prepared samples were kept at −20 °C until used (Wang et al., 2020b).

2.3. Dynamic interfacial pressure and interfacial viscoelasticity measurement of SPI and GSPI

The interfacial pressure and viscoelasticity were measured by contact angle measuring instrument (DSA100, KRUSS Scientific Instruments Co., Ltd., Hamburg, Germany) at 25 °C. The drop volume used in each sample was 10 μL and the adsorption time was 180 min. The amplitude and frequency were 10% and 0.1 Hz, respectively (Wang et al., 2020a).

2.4. Preparation of nanoemulsions for carrying β-carotene

An oil phase was prepared by dispersing 0.1% (w/v) β-carotene in soybean oil with mild heating at 50 °C for 5 min, and then was stirred at ambient temperature for about 3 h to ensure full dissolution. An aqueous phase was prepared by dispersing 0.5% (w/v) SPI or GSPI in deionized water. 5 mL oil phase and 95 mL aqueous phase were homogenized at 11, 000 rpm for 2 min with a high-speed shearer (FM200, FLUKO Shanghai Equipment Co., Ltd., Shanghai, China), and then the mixture was treated through a high-pressure homogenizer (AH-BASIC100, ATS Engineering Co., Ltd., Germany) at 500 bar for three times to prepare the nanoemulsions. The freshly prepared nanoemulsions were then sealed in aluminum foil covered glass tubes and stored at 4 °C (Salvia-Trujillo et al., 2013).

2.5. Particle size and Zeta potential measurement of emulsions

All samples were diluted 200-fold with deionized water. The particle size and Zeta-potential of the samples were detected using a Zetasizer Nano-ZS90 dynamic light scattering (DLS) instrument (Malvern Instruments, Worcestershire, UK), and each sample was tested three times (Liao et al., 2020). Instrument parameters: refraction rate 1.450, test temperature 25 °C, balance time 120 s.

2.6. The encapsulation efficiency and retention rate of β-carotene

β-Carotene in the nanoemulsions was extracted 3 times with ethanol and n-hexane solution (2:3, v/v). All the extracts were combined and the absorbance at 450 nm was measured by ultraviolet spectrophotometer (UV-1901, Beijing Purkinje General Instrument Co., Ltd., Beijing, China). The content of β-carotene in the samples was calculated according to the method described by Liu et al. (2021). Three groups of samples were taken for each nanoemulsion and were tested separately as parallel, and then the average value was taken.

$$\text{Encapsulation efficiency}\% = \frac{1 - \text{Free } \beta - \text{carotene content}}{\text{Total } \beta - \text{carotene content}} \times 100$$

$$\text{Retention rate}\% = \frac{\beta - \text{carotene content after storage } X \text{ d}}{\text{Total } \beta - \text{carotene content}} \times 100$$

X d represents the different storage time of samples.

2.7. Microstructure analysis of emulsions

The microstructure of emulsions was analyzed by a confocal laser scanning microscopy (CLSM) (TCS-SP5, Leica Microsystems Inc., Heidelberg, Germany). 20 μL of fluorescent dye (0.1% FITC and 0.1% Nile Red) was added to 5 mL emulsion, then the emulsion was incubated for 20 min at 4 °C in dark. 5 μL sample was dropped on one microscope slide and covered with a cover slip for microscopy. Images were immediately taken with a 40× magnification lens with excitation at 488 nm and 633 nm (Chen et al., 2020).

2.8. Establishment of the in vitro digestion model

A two stage digestion method in vitro was used to simulate the conditions of human stomach and intestine. 2 g NaCl and 7 mL HCl were dissolved in 1 L deionized water as simulated gastric reserve fluid. Before simulating gastric digestion, 10 mL of sample was mixed with 10 mL of simulated gastric reserve solution. The pH of the mixtures was adjusted to 2.0 by HCl dilution solution (0.1 mol/L), and then 32 mg pepsin was added. The mixtures were incubated in water bath at 37 °C for 1 h with stirring. After simulated gastric digestion, the pH of mixtures was quickly adjust to 7.0 by NaOH dilution solution (0.2 mol/L), then 10 mL of mixtures was mixed with 10 mL of simulated intestinal digestive juice (including 20 mg/mL bile salt and 1 mg/mL pancreatic enzyme). The mixtures were further incubated in water bath at 37 °C for 1 h with stirring (Yi et al., 2014).

2.8.1. Free fatty acid release rate

During simulated intestinal digestion, 0.25 mol/L NaOH was added constantly to keep the pH of digestive solution at 7.0. By recording the consumption of NaOH over time, the free fatty acid (FFA) release rate of lipid digestion can be calculated according to the following equation.

$$FFA\% = \frac{V_{NaOH} \times C_{NaOH} \times m_{lipid}}{W_{lipid} \times 2} \times 100\%$$

Where V_{NaOH} is the volume of NaOH required for titration (mL); C_{NaOH} is the concentration of used NaOH (0.25 mol/L); m_{lipid} is the molecular weight of oil (g/mol); W_{lipid} is the initial weight of oil.

2.8.2. Bioaccessibility of β-carotene

Digestive juices after simulated gastro-intestinal digestion were collected and ultracentrifuged at 4 °C with 10, 000 rpm for 30 min. The micellar phase of the interlayer was carefully separated using a syringe

and filtered with a 0.22 μm filter. The β-carotene in micellar phase was extracted and determined according to the method described in 2.6. Bioaccessibility was calculated according to the following equation.

$$\text{Bioaccessibility}\% = \frac{\beta - \text{carotene content in micelles}}{\beta - \text{carotene content in digesta}} \times 100\%$$

2.9. Statistical analysis

The data were analyzed and expressed as mean values ± standard deviation using SPSS software (Version 16.0, Chicago, IL, USA). The ANOVA of Duncan's multiple range test was used to evaluate the statistical significance of data, and the significance level was set at $P < 0.05$.

3. Results and discussion

3.1. Interfacial adsorption and dilatational rheological properties

3.1.1. Effects of glycation on adsorption kinetics of SPI

As can be seen from Fig. 1A, with the increase of adsorption time, the interface pressure (π) of SPI and GSPI increased rapidly in the early stage and then increased slowly. This indicated that the amphiphilic proteins could quickly diffuse to the oil-water interface in the early stage. But proteins at the interface might gradually become saturated as the number of proteins adsorbed at the interface increased (Seta et al., 2014). Moreover, the adsorbed proteins could undergo structural rearrangement at the interface, which hindered the continued adsorption of proteins (Baldursdottir et al., 2010). Compared with SPI, the interface pressure of GSPI at oil-water interface was weaker. In this study, the grafting degrees of SPI with glucose, lactose, galactose oligosaccharide and dextran were 31.42%, 43.84%, 39.65% and 39.80%, respectively. The introduction of sugar chain could reduce the hydrophobic groups of soybean protein. Meanwhile, sugar chain in water phase can also prevent the movement of soybean protein to the oil-water interface. So, the interface pressure of GSPI decreased.

The adsorption kinetics parameters of protein include diffusion rate (K_{diff}), permeation rate (K_p) and rearrangement rate (K_r). They are calculated by fitting, regressing, or just the line-slope from some selected points in Fig. 1. As shown in Fig. 1B and C, these parameters can be obtained by analyzing changes of interface pressure in a specific time through Ward-Tordai equation and the first-rate equation (Xiong et al., 2018). The results are shown in Table 1. Compared with SPI, the diffusion rate of glycated soybean protein decreased at the oil-water interface, but the permeate and rearrangement rate increased. This might be due to the fact that the covalent grafting of reducing sugars shielded the hydrophobic groups on the surface of SPI or provided a strong steric hindrance effect, thus limiting the adsorption of protein molecules at the oil-water interface (Dong and Hua, 2018). Meanwhile, the conformational changes of protein also affected its adsorption at the oil-water interface. Unmodified SPI contained more globulins with small molecular weight, which were easily adsorbed at the oil-water interface and exposed more hydrophobic groups. After glycation modification, the adsorption process of protein was slowed down due to the presence

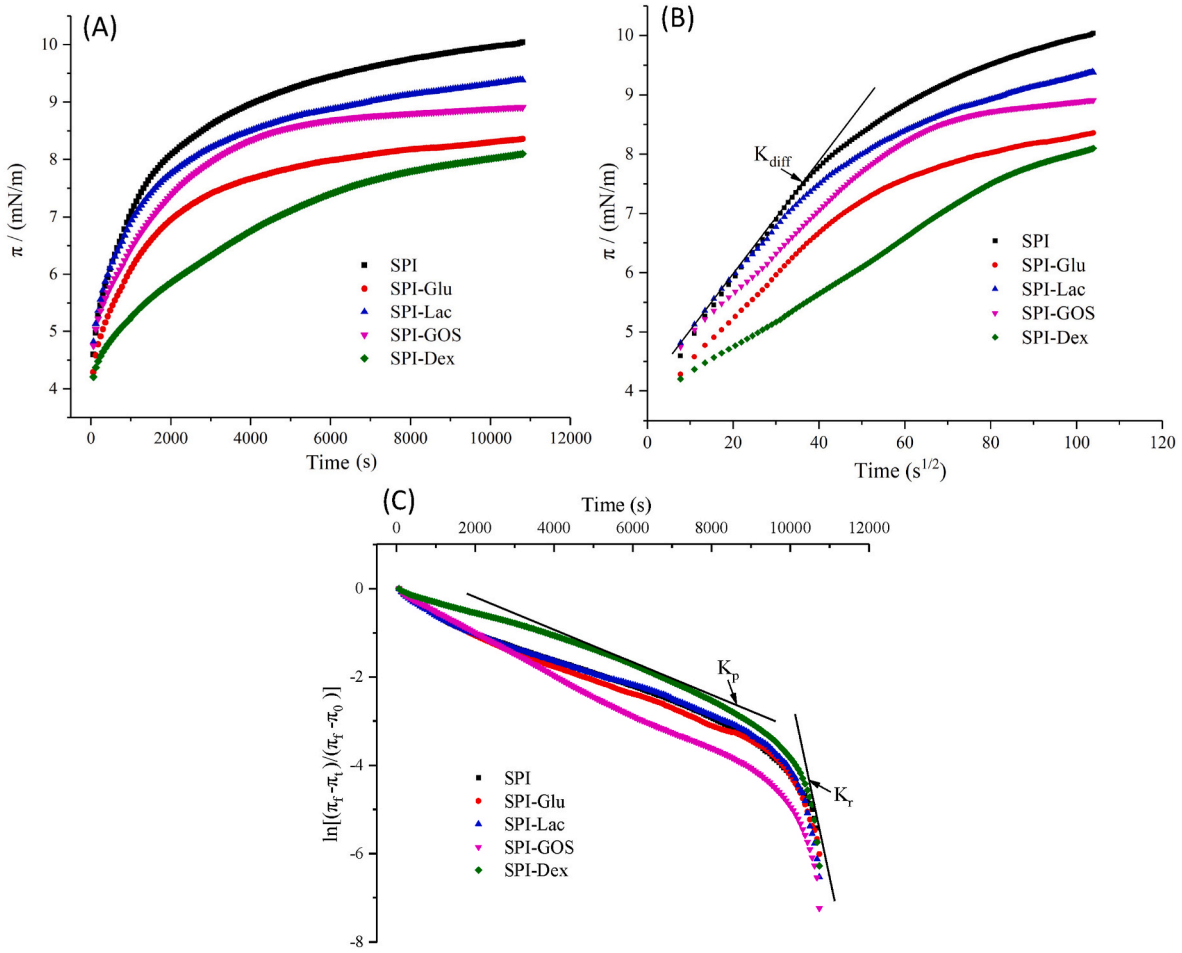

Fig. 1. (A) Time dependence of interfacial pressure (π) for SPI and GSPI adsorbed films at the oil-water interface. (B) Square root of time ($t^{1/2}$) dependence of interfacial pressure (π) for SPI and GSPI adsorbed films at the oil-water interface. K_{diff} represents diffusion rate. (C) Typical profile of molecular permeation and structural rearrangement steps at the oil-water interface for SPI and GSPI. K_p represents permeation rate, K_r represents rearrangement rate.

Table 1
Interface adsorption kinetics parameters of SPI and GSPI.

Samples	$K_{diff} \times 10^2/(mN/m/s^{1/2})$ (R^2)	$K_p \times 10^4/(s^{-1})$ (R^2)	$K_r \times 10^3/(s^{-1})$ (R^2)
SPI	8.754 ± 0.151 (0.9879)	−2.963 ± 0.007 (0.9996)	−1.966 ± 0.192 (0.9454)
SPI-Glu	6.874 ± 0.069 (0.9959)	−3.069 ± 0.007 (0.9997)	−2.724 ± 0.138 (0.9824)
SPI-Lac	7.345 ± 0.125 (0.9882)	−2.747 ± 0.011 (0.9990)	−4.090 ± 0.236 (0.9773)
SPI-GOS	6.968 ± 0.029 (0.9993)	−4.545 ± 0.029 (0.9974)	−3.517 ± 0.402 (0.9163)
SPI-Dex	4.458 ± 0.018 (0.9994)	−3.304 ± 0.025 (0.9962)	−4.086 ± 0.502 (0.9043)

Note: K_{diff} is the diffusion rate; K_P is the permeation rate; Kr is the rearrangement rate.

of sugar chains, and each molecule occupied a larger interface area. Moreover, the spatial structure of glycated soybean protein became disordered and conformational flexibility increased, which was conducive to the unfolding and rearrangement of protein molecules at the interface (Tian et al., 2020).

3.1.2. *Effects of glycation on interface dilatational viscoelasticity of SPI*

The dilatational viscoelasticity can reflect the resisting external deformation ability of the interfacial film, which is usually related to the interaction between interfacial molecules (Maldonado-Valderrama and Patino, 2010). The slope of interfacial expansion modulus (E) and interfacial pressure (π) curve is generally used to analyze the degree of intermolecular interaction (Rodriguez Patino et al., 2003). It was found that the interfacial expansion modulus of all samples increased with the increase of adsorption time (Fig. 2A), indicating that intermolecular interaction was formed after protein was adsorbed to the interface. The interfacial film formed by GSPI had the higher interfacial expansion modulus with the adsorption time of more than 150 min. These results indicated that glycation improved the viscoelasticity of the protein interface film and made it more resistant to external deformation, which was beneficial to the long-term stability of the emulsion (Wang et al., 2020a).

According to Fig. 2B, the slopes of E-π curve of all samples were greater than 1.0. This manifested that there was a strong interaction between molecules, which was in a serious non-ideal behavior (Romero et al., 2011). The slopes of E-π curve of GSPI were larger than that of SPI, indicated that the interaction of interface proteins was enhanced after glycation. This may be due to the greater molecular flexibility of GSPI which can fully unfold and rearrange at the oil-water interface (Li et al., 2019). The change of tangent value of phase angle (tan δ) with adsorption time, which was equal to the ratio of viscous modulus to elastic modulus, was presented in Fig. 2C. It could be found that the tan δ values of almost all samples were less than 0.4 and decreased gradually with the extension of adsorption time. This indicated that the interfacial film formed by protein had high elasticity, and the elastic modulus of the interfacial film gradually increased with the increase of adsorption time.

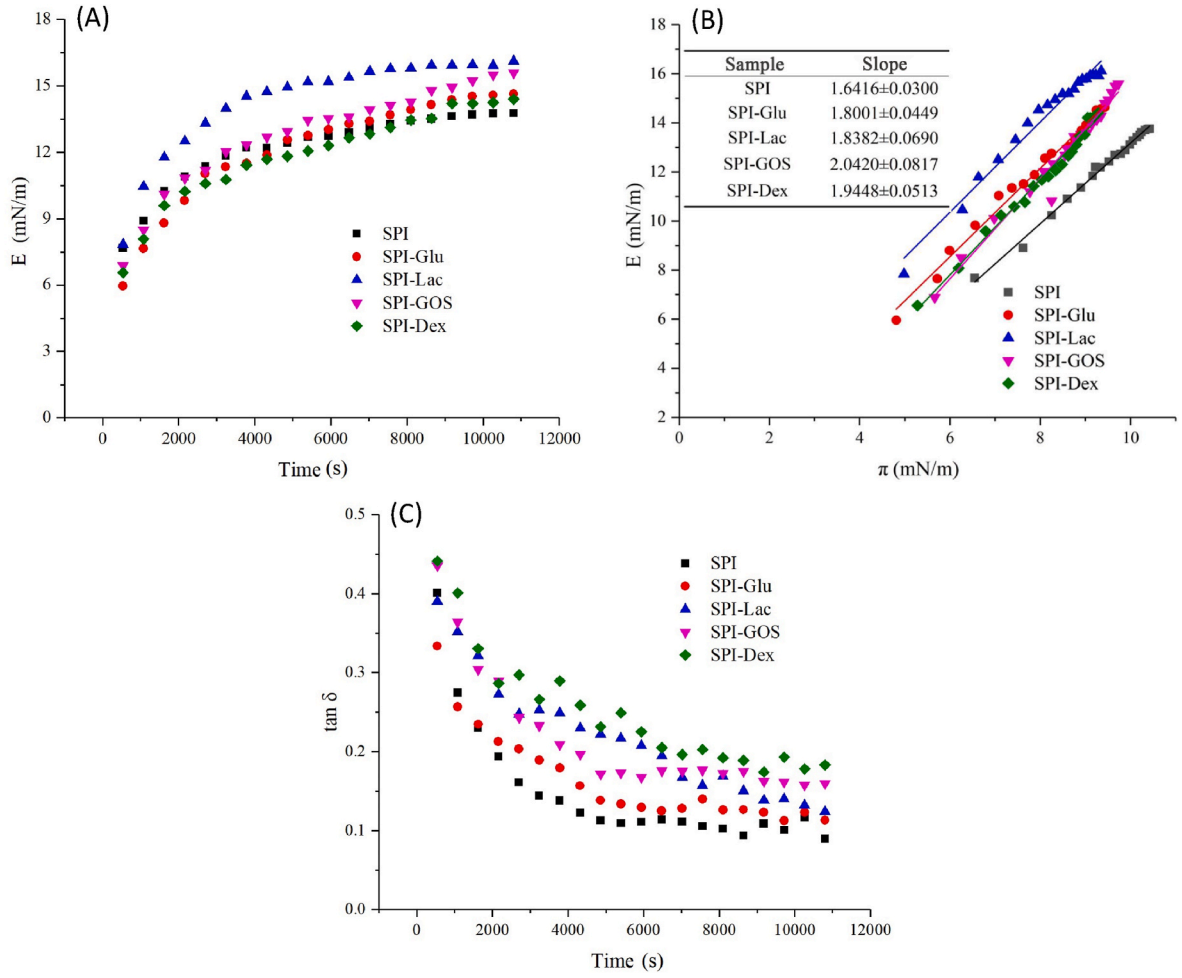

Fig. 2. (A) Interfacial expansion modulus (E) as a function of adsorption time for SPI and GSPI adsorbed films at the oil-in-water interface. (B) Interfacial expansion modulus (E) as a function of interfacial pressure (π) for SPI and GSPI adsorbed films at the oil-in-water interface. (C) Time-dependent phase angle tangent (tan δ) for SPI and GSPI adsorbed films at the oil-in-water interface.

3.2. Effects of glycation on the properties of β-carotene nanoemulsions

The properties of β-carotene nanoemulsions formed from SPI and GSPI are showed in Table 2. The polymer dispersity index (PDI) values of all emulsions were around 0.2 (Table 2), indicating that the nanoemulsions obtained by high pressure homogenization had good dispersion property. Compared with the SPI, the average particle size of GSPI stabilized nanoemulsions decreased significantly, and the absolute value of Zeta potential increased significantly. The results indicated that glycation modification increased the electrostatic repulsion between the droplets. Meanwhile, the introduction of sugar chain also increased the thickness of the interface film, which was beneficial to the stability between the droplets (Liu et al., 2018). Compared with SPI, GSPI had the higher encapsulation efficiency of more than 94%, indicating the good emulsifying properties of GSPI.

3.3. Effects of glycation on storage stability of β-carotene nanoemulsions

Due to thermodynamic instability, nanoemulsions are prone to be unstable under adverse environmental conditions. This is a challenge for the delivery of bioactive substances. Therefore, the physical stability and β-carotene retention of nanoemulsions stored at 4 °C and 25 °C for 28 days were evaluated.

3.3.1. The particle size and Zeta potential changes of nanoemulsions during storage

As shown in Fig. 3A and B, the average particle size of the emulsion increased with the prolonging of storage days. The average particle size of SPI stabilized nanoemulsions was below 600 nm during storage at 4 °C, after 14 days storage at 25 °C, the particle size increased significantly, reaching about 3000 nm at 28 days. However, the average particle size of GSPI stabilized nanoemulsions remained below 500 nm at 4 °C and 25 °C during the whole storage. These results indicated that GSPI stabilized nanoemulsions had good physical stability, which could resist the flocculation of oil droplets during the long-term storage. In addition, the larger the molecular weight of grafted sugar was, the smaller the change of average particle size was, indicating that the nanoemulsions formed by SPI-dextran complex had better storage stability.

It was found from Fig. 3C and D that the charged amount of the emulsion was reduced during storage. Notably, the charge of SPI nanoemulsions was reduced by about half after storage for 28 days at 25 °C. The absolute values of Zeta potential of GSPI nanoemulsions were higher than those of SPI nanoemulsions. This indicated that in SPI emulsions the electrostatic repulsion between droplets gradually weakened with the prolonging of storage time and increase of temperature, which was not conducive to the stability of the emulsion. After glycation, the covalently grafted sugar chain on protein molecule increased the surface charge and provided a certain steric repulsion. Therefore, the glycated protein could maintain the balance between the droplets during storage and prevent droplet aggregation.

Fig. 3E and F showed that the particle size distribution of all emulsions was relatively uniform after 28 days storage at 4 °C. The particle size distribution of SPI nanoemulsions moved significantly in the direction of larger particle size at 25 °C, while GSPI emulsions tended to the direction of smaller particle size. Higher storage temperatures could speed up the movement of oil droplets and increase the probability of collisions between oil droplets, resulting in the formation of large oil droplets (Borba et al., 2019). However, glycation could effectively reduce the collision of oil droplets by introducing sugar chains as the shells of droplets or increasing the electrostatic repulsion between the droplets (Zhang et al., 2019). Thus, the GSPI emulsion can maintain stable properties even under adverse storage conditions.

Table 2
Properties of β-carotene nanoemulsions stabilized by SPI and GSPI.

Samples	Average particle size (nm)	PDI	Zeta potential (mV)	Encapsulation efficiency (%)
SPI	333.77 ± 7.50^{a}	0.21 ± 0.02^{ab}	-38.23 ± 0.71^{a}	89.90 ± 1.01^{c}
SPI-Glu	280.80 ± 2.34^{c}	0.21 ± 0.02^{ab}	-50.17 ± 1.07^{c}	96.09 ± 0.50^{ab}
SPI-Lac	294.77 ± 2.99^{b}	0.24 ± 0.00^{a}	-49.27 ± 0.67^{c}	94.31 ± 1.61^{b}
SPI-GOS	289.20 ± 2.43^{bc}	0.18 ± 0.04^{b}	-49.33 ± 0.86^{c}	97.44 ± 0.60^{a}
SPI-Dex	282.80 ± 5.06^{c}	0.22 ± 0.03^{ab}	-45.80 ± 0.56^{b}	97.51 ± 0.91^{a}

Note: Means ± standard deviations of triplicate analyses are given. Different superscript letters indicate a significant difference between the same column of data ($P < 0.05$).

3.3.2. The microstructure of nanoemulsions during storage

The microstructure of nanoemulsions after 28 days of storage was shown in Fig. 4. The nanoemulsions still maintained a good dispersion state under low temperature storage (4 °C), and there was no large amount of flocculation between oil droplets. However, large oil droplets appeared in the SPI nanoemulsions under high storage temperature (25 °C), and obvious flocculation phenomenon occurred. The droplets in GSPI nanoemulsions were still evenly distributed. The results were consistent with Fig. 3, indicating that glycated protein could effectively improve the storage stability of nanoemulsions.

3.3.3. The retention rate changes of β-carotene during storage

β-Carotene is easily degraded by oxidation in air due to its conjugated unsaturated double bond (Boon et al., 2010). As shown in Fig. 5, β-carotene retention rate of all nanoemulsions decreased to varying degrees during storage at 4 °C and 25 °C. During storage at 4 °C, the β-carotene retention rate of the emulsions basically remained above 95%. After storage at 4 °C for 28 days, the β-carotene retention rate of GSPI nanoemulsions was significantly higher than that of SPI nanoemulsions ($P < 0.05$). During storage at 25 °C, β-carotene was greatly lost. The β-carotene retention rate of SPI nanoemulsions was only 63% after 28 days storage at 25 °C, while the retention rate of β-carotene in GSPI nanoemulsions was basically above 80%. The protective effect of GSPI on β-carotene in nanoemulsion system was stronger than that of SPI. On the one hand, glycated protein can form a thick interface film to prevent the diffusion of dissolved oxygen and free radicals on the interface. On the other hand, it may also be related to the high antioxidant effect of glycated products (Jia et al., 2020).

3.4. Effects of digestion in vitro on physicochemical properties of nanoemulsions

3.4.1. The particle size and Zeta potential changes of nanoemulsions after the in vitro digestion

As shown in Fig. 6A, compared with the initial emulsion, the average particle size of the emulsion increased significantly after entering the stomach phase. The average particle size of GSPI stabilized emulsion was significantly lower than that of SPI stabilized emulsion. The interfacial protein was hydrolyzed by pepsin and the interfacial membrane structure of droplets was destroyed in the process of simulated gastric digestion, resulting in the aggregation of droplets (Yao et al., 2013). The steric hindrance effect of glycated protein can block pepsin adsorption and weaken the hydrolysis of interfacial protein, thus protecting the structure of emulsion from damage (Zhong et al., 2019). Subsequently, the average particle size of nanoemulsions decreased greatly during intestinal digestion. This may be due to the fact that in intestinal digestion bile salts with high surface activity can replace the interface molecules and compete with emulsifiers for adsorption, resulting in the formation of smaller droplets.

After simulated gastric digestion, the absolute value of Zeta potential decreased significantly (Fig. 6B), which might be due to the electrostatic

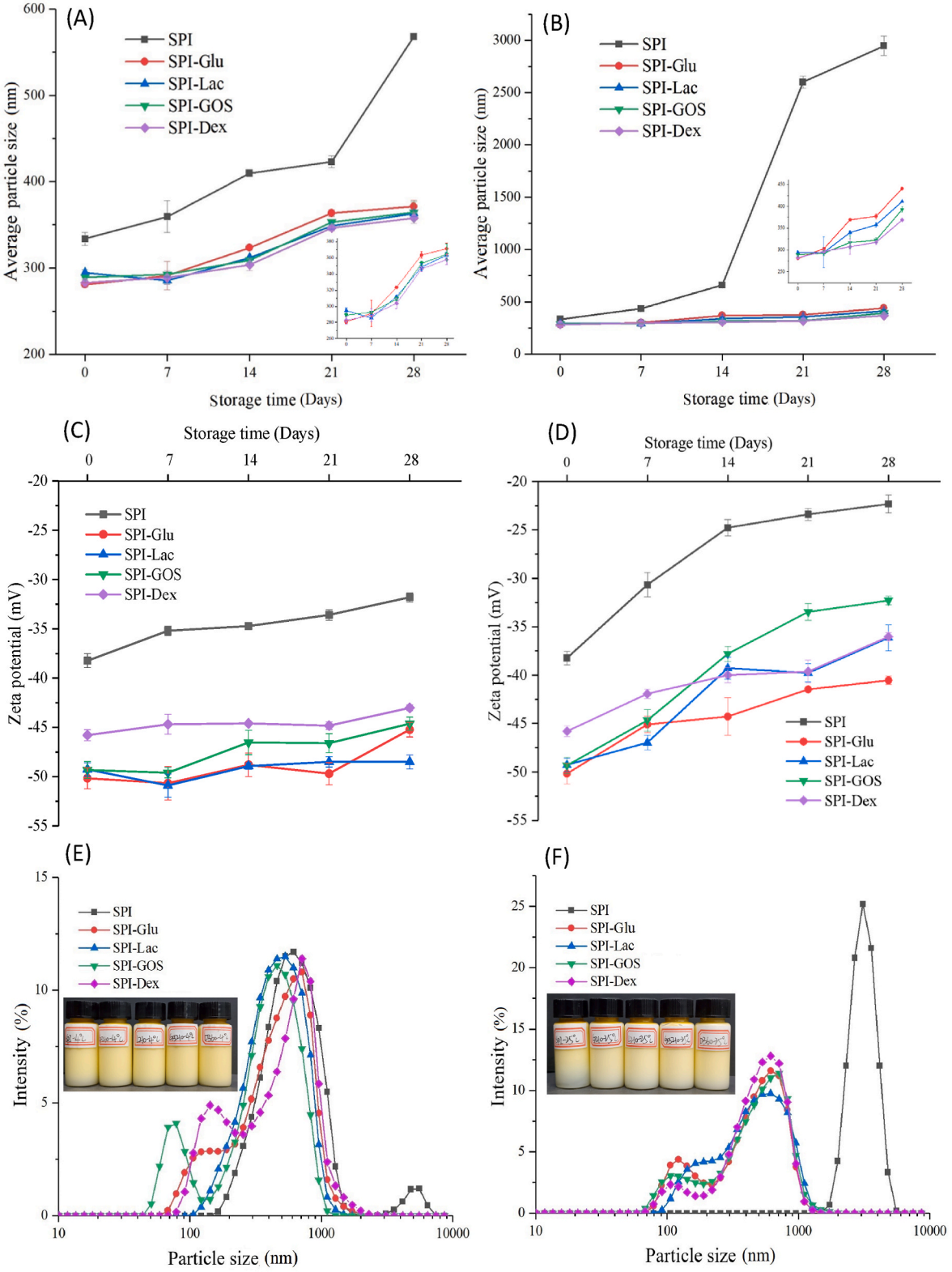

Fig. 3. Effects of glycated protein on the physical stability of nanoemulsions during 28 days storage. Average particle size: (A) 4 °C; (B) 25 °C. Zeta potential: (C) 4 °C; (D) 25 °C. Particle size distribution after 28 days of storage: (E) 4 °C; (F) 25 °C.

shielding effect caused by high ionic strength in simulated gastric juice or the hydrolysis of pepsin (Nik et al., 2011). After the simulation of intestinal digestion, the absolute value of Zeta potential increased significantly again, which might be related to the replacement of protein hydrolysate at the interface by bile salts and fatty acids released by lipid hydrolysis (Chen et al., 2020). In addition, after simulated gastrointestinal digestion, the absolute value of Zeta potential of GSPI nanoemulsions was generally higher than that of SPI nanoemulsions, indicated that glycated soybean protein could increase the electrostatic repulsion between molecules and improve emulsion stability.

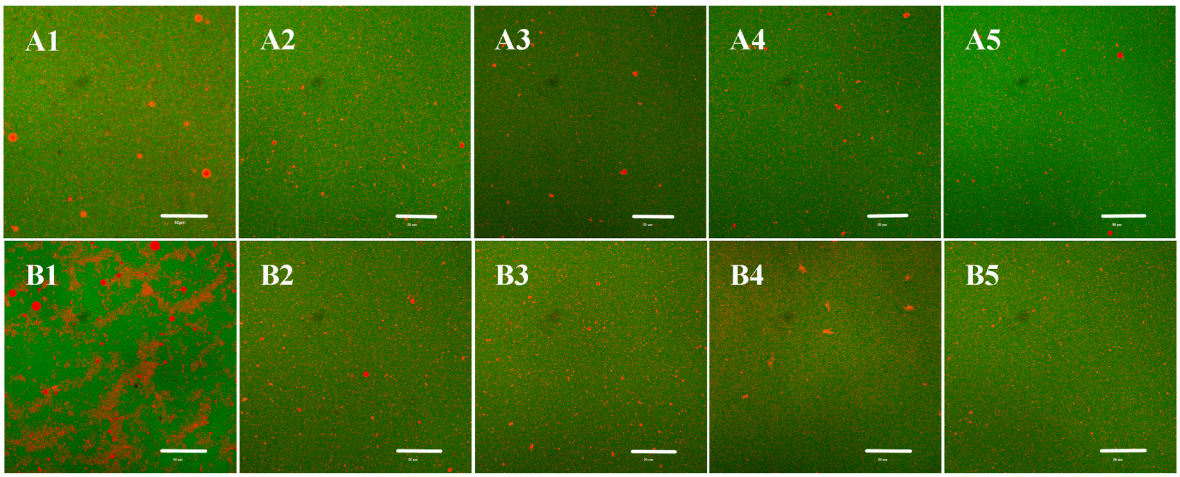

Fig. 4. CLSM images of nanoemulsions after 28 days of storage at 4 °C (A) and 25 °C (B). 1: nanoemulsion stablized by SPI; 2–5: nanoemulsions stablized by SPI-Glu, SPI-Lac, SPI-GOS and SPI-Dex, respectively. The white scale bar in the figure represents 50 μm.

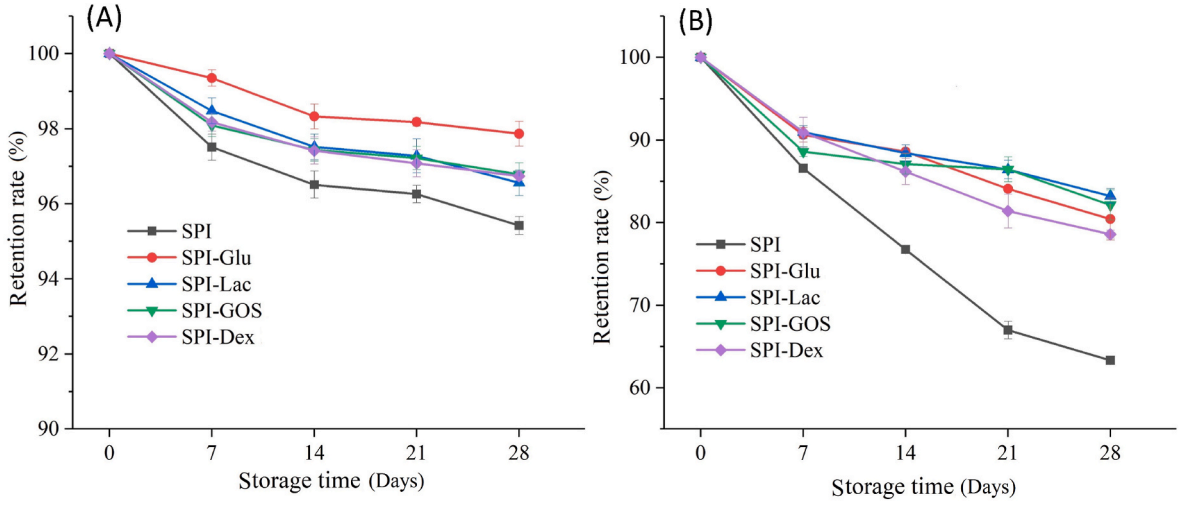

Fig. 5. Effects of glycated protein on the retention rate of β-carotene in nanoemulsions during 28 days storage at 4 °C (A) and 25 °C (B).

3.4.2. The microstructure of nanoemulsions after the in vitro digestion

It could be seen from Fig. 7 that the formation of large oil droplets was observed in SPI emulsion after simulating digestion of gastric juice, and flocculation phenomenon occurred between the droplets. In comparison, the droplet size of GSPI emulsion in simulated stomach phase was relatively small and more uniform, which was almost consistent with the detection results of average particle size. It indicated that the structure of interface protein in SPI emulsion was destroyed greatly due to pepsin digestion, and small oil droplets fused with each other to form large oil droplets. In contrast, pepsin had less damage to the interface protein after glycation modification, and the GSPI nanoemulsions still had a large interface area after simulated gastric juice digestion. It was observed that the number and size of oil droplets decreased significantly after simulated intestinal digestion, indicating that most of the oil droplets were hydrolyzed by lipase during the process of simulating intestine digestion.

3.4.3. The free fatty acid release of nanoemulsions after the in vitro digestion

As shown in Fig. 8, the free fatty acid (FFA) release rate increased rapidly within 25 min of simulated intestinal digestion. With the prolongation of digestion time, the FFA release rate increased slowly, and reached a stable state after 30 min of simulated intestinal digestion. This phenomenon indicated that bile salt and lipase adsorbed quickly to the surface of oil droplets at the initial intestinal digestion stage, promoting oil digestion (Infantes-Garcia et al., 2021). Then bile salts on the oil-water interface tended to saturate gradually, and the free fatty acids generated by lipolysis also competed and adsorbed to the interface, preventing the contact between lipase and oil droplets (Lv et al., 2019). In addition, it also could be found from Fig. 8 that the FFA release rate of GSPI nanoemulsions was higher than that of SPI, and increased with the increase of molecular weight of reducing sugars. This might be related to the fact that the average particle size of GSPI nanoemulsions was significantly lower than that of SPI after gastric juice digestion (Fig. 6A), and then in the simulated intestinal digestion, GSPI nanoemulsions had a larger specific surface area, which could absorb more bile salts and lipase, thus releasing more FFAs (Salvia-Trujillo et al., 2013).

3.4.4. Bioaccessibility of β-carotene in nanoemulsions

The bioaccessibility of β-carotene was positively correlated with the final free fatty acid release rate of nanoemulsions. It can be seen from Fig. 9, in GSPI nanoemulsions, the bioaccessibility of β-carotene was above 70%, which was significantly higher than that of β-carotene in SPI nanoemulsions. Especially, in the nanoemulsions formed by SPI-dextran complex, β-carotene had the highest bioaccessibility. After simulated gastric digestion, glycated proteins might be more easily replaced by bile

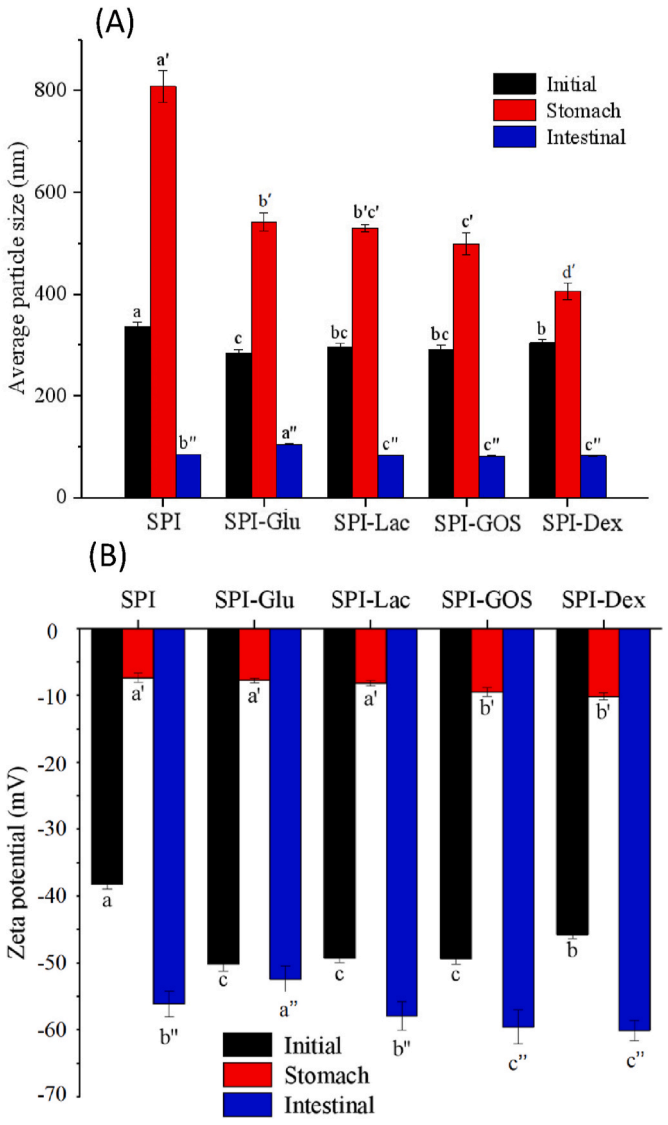

Fig. 6. The average particle size (A) and Zeta potential (B) of nanoemulsions in different digestion phases. Different letters indicate significant differences in values among samples at various treatments ($P < 0.05$).

salts, thus providing more action sites for pancreatic lipase (Liu et al., 2020). Free fatty acids released by lipid hydrolysis and bile salts can form mixed micelles with hydrophobic domains. So, the more free fatty acids were eventually released, the more mixed micelles were produced. The micelles could dissolve β-carotene and allow it to be absorbed and utilized by intestinal epithelial cells (Yi et al., 2015). In addition, the introduction of sugar chain could effectively protect the droplets structure in GSPI nanoemulsions from being damaged by gastric juice. Therefore, they had a larger specific surface area when they reached the small intestine, which was conducive to the adsorption of bile salt and lipase (Salvia-Trujillo and McClements, 2016). Consequently, the GSPI nanoemulsions could transfer more β-carotene into the mixed micelles, thus improved the bioaccessibility of β-carotene.

4. Conclusions

In this study, SPI was glycated with four reducing sugars of different molecular weights. The permeability and rearrangement rate of SPI after glycation increased at the oil-water interface, which enhanced the interfacial protein interaction and the viscoelasticity of interface film. In GSPI nanoemulsions, the encapsulation efficiency and storage stability

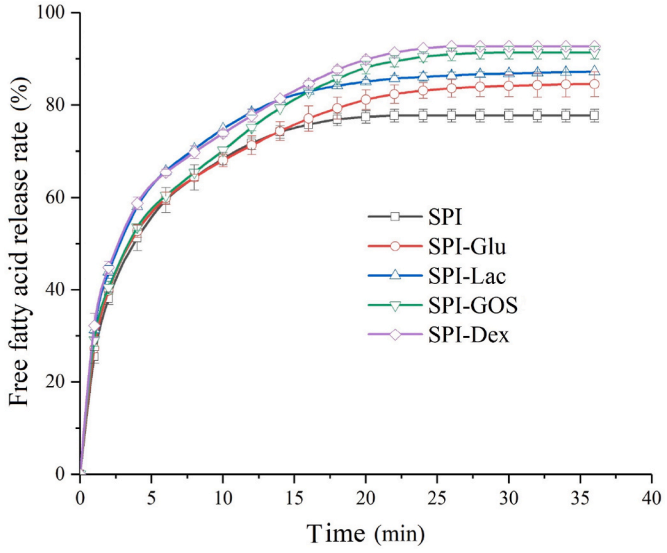

Fig. 8. The free fatty acid release rate in nanoemulsions during simulated intestinal digestion.

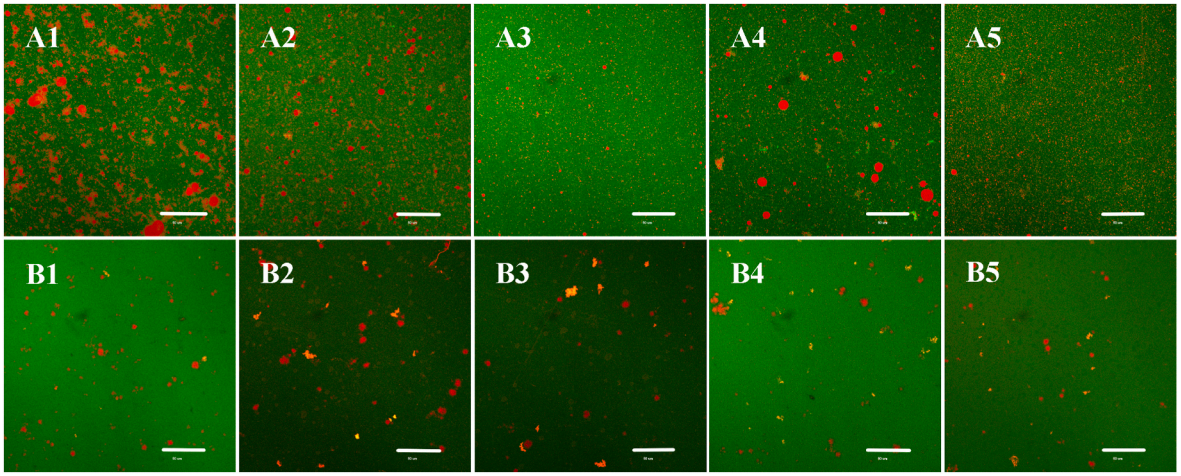

Fig. 7. CLSM images of nanoemulsions after the in vitro digestion. (A): simulated gastric digestion; (B): simulated intestinal digestion. 1: nanoemulsion stablized by SPI; 2–5: nanoemulsions stablized by SPI-Glu, SPI-Lac, SPI-GOS and SPI-Dex, respectively. The white scale bar in the figure represents 50 μm.

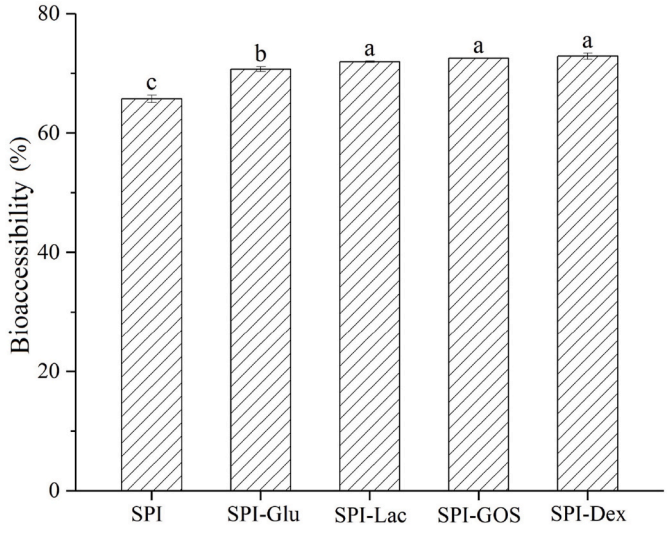

Fig. 9. The bioaccessibility of β-carotene in nanoemulsions after the in vitro digestion. Different letters indicate significant differences in values among samples ($P < 0.05$).

were improved, and the improvement effect of dextran glycation was the best. During the in vitro gastrointestinal digestion, the GSPI nanoemulsions had higher interface area after entering intestine digestion, which could improve the free fatty acid release rate and increase the bioaccessibility of β-carotene. Therefore, glycated soybean protein could been used to prepare nanoemulsions with better stability, and could effectively increase the bioavailability of β-carotene. The study provides theoretical basis for the application of glycated soybean protein nanoemulsions in the delivery system of β-carotene and other fat-soluble bioactive substances.

Credit author statement

Guanhao Bu: Conceptualization, Methodology, Resources, Formal analysis, Supervision, Writing - review & editing. Chenyu Zhao: Conceptualization, Methodology, Software, Investigation, Data curation, Writing - original draft. Meiyue Wang: Visualization, Validation. Zhen Yu, Hongshun Yang and Tingwei Zhu: Writing - review & editing.

Declaration of competing interest

The authors declare that they have no known competing financial interests or personal relationships that could have appeared to influence the work reported in this paper.

Data availability

Data will be made available on request.

Acknowledgements

This work was supported by the National Natural Science Foundation of China (31871748, 31201293), the Young-aged Backbone Teacher Funds of Henan Province of China (2019GGJS084), the Project of Henan University of Technology Excellent Young Teachers (21420064), the Zhengzhou Science and Technology Collaborative Innovation Project (21ZZXTCX17), the China Postdoctoral Science Foundation (2021M701112), the Innovative Funds Plan of Henan University of Technology (2021ZKCJ03), and the State Scholarship Fund from China Scholarship Council (202008410099).

References

Afonso, B.S., Azevedo, A.G., Goncalves, C., Amado, I.R., Ferreira, E.C., Pastrana, L.M., Cerqueira, M.A., 2020. Bio-based nanoparticles as a carrier of beta-carotene: production, characterisation and in vitro gastrointestinal digestion. Molecules 25 (19), 4497. https://doi.org/10.3390/molecules25194497.

Baldursdottir, S.G., Fullerton, M.S., Nielsen, S.H., Jorgensen, L., 2010. Adsorption of proteins at the oil/water interface-observation of protein adsorption by interfacial shear stress measurements. Colloids Surf. B Biointerfaces 79 (1), 41–46. https://doi.org/10.1016/j.colsurfb.2010.03.020.

Bhushani, J.A., Karthik, P., Anandharamakrishnan, C., 2016. Nanoemulsion based delivery system for improved bioaccessibility and Caco-2 cell monolayer permeability of green tea catechins. Food Hydrocolloids 56, 372–382. https://doi.org/10.1016/j.foodhyd.2015.12.035.

Boon, C.S., Mcclements, D.J., Weiss, J., Decker, E.A., 2010. Factors influencing the chemical stability of carotenoids in foods. Crit. Rev. Food Sci. Nutr. 50 (6), 515–532. https://doi.org/10.1080/10408390802565889.

Boostani, S., Aminlari, M., Moosavi-Nasab, M., Niakosari, M., Mesbahi, G., 2017. Fabrication and characterisation of soy protein isolate-grafted dextran biopolymer: a novel ingredient in spray-dried soy beverage formulation. Int. J. Biol. Macromol. 102, 297–307. https://doi.org/10.1016/j.ijbiomac.2017.04.019.

Borba, C.M., Tavares, M.N., Macedo, L.P., Araujo, G.S., Furlong, E.B., Dora, C.L., Burkert, J.F.M., 2019. Physical and chemical stability of β-carotene nanoemulsions during storage and thermal process. Food Res. Int. 121, 229–237. https://doi.org/10.1016/j.foodres.2019.03.045.

Caballero, S., Davidov-Pardo, G., 2021. Comparison of legume and dairy proteins for the impact of maillard conjugation on nanoemulsion formation, stability, and lutein color retention. Food Chem. 338, 128083 https://doi.org/10.1016/j.foodchem.2020.128083.

Chen, L., Yokoyama, W., Liang, R., Zhong, F., 2020. Enzymatic degradation and bioaccessibility of protein encapsulated β-carotene nano-emulsions during in vitro gastro-intestinal digestion. Food Hydrocolloids 100, 105177. https://doi.org/10.1016/j.foodhyd.2019.105177.

Chen, L.L., Bai, G.L., Yang, R., Zang, J.C., Zhou, T., Zhao, G.H., 2014. Encapsulation of beta-carotene within ferritin nanocages greatly increases its water-solubility and thermal stability. Food Chem. 149, 307–312. https://doi.org/10.1016/j.foodchem.2013.10.115.

Corredig, M., Sharafbafi, N., Kristo, E., 2011. Polysaccharide-protein interactions in dairy matrices, control and design of structures. Food Hydrocolloids 25 (8), 1833–1841. https://doi.org/10.1016/j.foodhyd.2011.05.014.

Dong, D., Hua, Y.F., 2018. Emulsifying behaviors and interfacial properties of different protein/gum Arabic complexes: effect of pH. Food Hydrocolloids 74, 289–295. https://doi.org/10.1016/j.foodhyd.2017.08.014.

Donhowe, E.G., Kong, F.B., 2014. Beta-carotene: digestion, microencapsulation, and in vitro bioavailability. Food Bioprocess Technol. 7 (2), 338–354. https://doi.org/10.1007/s11947-013-1244-z.

Haskell, M.J., 2012. The challenge to reach nutritional adequacy for vitamin A: β-carotene bioavailability and conversion-evidence in humans. Am. J. Clin. Nutr. 96 (5), 1193S–1203S. https://doi.org/10.3945/ajcn.112.034850.

Infantes-Garcia, M.R., Verkempinck, S.H.E., Gonzalez-Fuentes, P.G., Hendrickx, M.E., Grauwet, T., 2021. Lipolysis products formation during in vitro gastric digestion is affected by the emulsion interfacial composition. Food Hydrocolloids 110, 106163. https://doi.org/10.1016/j.foodhyd.2020.106163.

Jia, C.S., Cao, D.D., Ji, S.P., Lin, W.T., Zhang, X.M., Muhoza, B., 2020. Whey protein isolate conjugated with xylo-oligosaccharides via maillard reaction: characterization, antioxidant capacity, and application for lycopene microencapsulation. LWT–Food Sci. Technol. 118, 108837 https://doi.org/10.1016/j.lwt.2019.108837.

Kong, L.Y., Bhosale, R., Ziegler, G.R., 2018. Encapsulation and stabilization of beta-carotene by amylose inclusion complexes. Food Res. Int. 105, 446–452. https://doi.org/10.1016/j.foodres.2017.11.058.

Lesmes, U., McClements, D.J., 2012. Controlling lipid digestibility: response of lipid droplets coated by beta-lactoglobulin-dextran maillard conjugates to simulated gastrointestinal conditions. Food Hydrocolloids 26 (1), 221–230. https://doi.org/10.1016/j.foodhyd.2011.05.011.

Li, R., Cui, Q., Wang, G., Liu, J., Chen, S., Wang, X., Wang, X., Jiang, L., 2019. Relationship between surface functional properties and flexibility of soy protein isolate-glucose conjugates. Food Hydrocolloids 95, 349–357. https://doi.org/10.1016/j.foodhyd.2019.04.030.

Liao, Y.M., Zhong, L., Liu, L.N., Xie, L., Tang, H.L., Zhang, L.L., Li, X.F., 2020. Comparison of surfactants at solubilizing, forming and stabilizing nanoemulsion of hesperidin. J. Food Eng. 281, 110000 https://doi.org/10.1016/j.jfoodeng.2020.110000.

Liu, C., Wang, Z.J., Jin, H., Wang, X.Y., Gao, Y., Zhao, Q.S., Liu, C.H., Xu, J., 2020. Effect of enzymolysis and glycosylation on the curcumin nanoemulsions stabilized by beta-conglycinin: formation, stability and in vitro digestion. Int. J. Biol. Macromol. 142, 658–667. https://doi.org/10.1016/j.ijbiomac.2019.10.007.

Liu, Y., Yadav, M.P., Yin, L.J., 2018. Enzymatic catalyzed corn fiber gum-bovine serum albumin conjugates: their interfacial adsorption behaviors in oil-in-water emulsions. Food Hydrocolloids 77, 986–994. https://doi.org/10.1016/j.foodhyd.2017.11.048.

Liu, Y.L., Liu, C., Zhang, S.Y., Li, J.S., Zheng, H.Y., Jin, H., Xu, J., 2021. Comparison of different protein emulsifiers on physicochemical properties of beta-carotene-loaded nanoemulsion: effect on formation, stability, and in vitro digestion. Nanomaterials 11 (1), 167. https://doi.org/10.3390/nano11010167.

Lv, S.S., Zhang, Y.H., Tan, H.Y., Zhang, R.J., McClements, D.J., 2019. Vitamin E encapsulation within oil-in-water emulsions: impact of emulsifier type on

physicochemical stability and bioaccessibility. J. Agric. Food Chem. 67 (5), 1521–1529. https://doi.org/10.1021/acs.jafc.8b06347.
Ma, X., Yan, T., Miao, S., Mao, L., Liu, D., 2022. In vitro digestion and storage stability of β-carotene-loaded nanoemulsion stabilized by soy protein isolate (SPI)-citrus pectin (CP) complex/conjugate prepared with ultrasound. Foods 11, 2410. https://doi.org/10.3390/foods11162410.
Maldonado-Valderrama, J., Patino, J.M.R., 2010. Interfacial rheology of protein-surfactant mixtures. Curr. Opin. Colloid Interface Sci. 15 (4), 271–282. https://doi.org/10.1016/j.cocis.2009.12.004.
Nik, A.M., Wright, A.J., Corredig, M., 2011. Micellization of beta-carotene from soy-protein stabilized oil-in-water emulsions under in vitro conditions of lipolysis. J. Am. Oil Chem. Soc. 88 (9), 1397–1407. https://doi.org/10.1007/s11746-011-1806-z.
Peng, X.Q., Xu, Y.T., Liu, T.X., Tang, C.H., 2018. Molecular mechanism for improving emulsification efficiency of soy glycinin by glycation with soy soluble polysaccharide. J. Agric. Food Chem. 66, 12316–12326. https://doi.org/10.1021/acs.jafc.8b03398.
Rodriguez Patino, J.M., Molina Ortiz, S.E., Carrera Sanchez, C., Rodriguez Nino, M.R., Anon, M.C., 2003. Dynamic properties of soy globulin adsorbed films at the air-water interface. J. Colloid Interface Sci. 268 (1), 50–57. https://doi.org/10.1016/S0021-9797(03)00642-8.
Romero, A., Beaumal, V., David-Briand, E., Cordobes, F., Guerrero, A., Anton, M., 2011. Interfacial and oil/water emulsions characterization of potato protein isolates. J. Agric. Food Chem. 59 (17), 9466–9474. https://doi.org/10.1021/jf2019853.
Salvia-Trujillo, L., McClements, D.J., 2016. Enhancement of lycopene bioaccessibility from tomato juice using excipient emulsions: influence of lipid droplet size. Food Chem. 210, 295–304. https://doi.org/10.1016/j.foodchem.2016.04.125.
Salvia-Trujillo, L., Qian, C., Martin-Belloso, O., McClements, D.J., 2013. Influence of particle size on lipid digestion and beta-carotene bioaccessibility in emulsions and nanoemulsions. Food Chem. 141 (2), 1472–1480. https://doi.org/10.1016/j.foodchem.2013.03.050.
Semenova, M., 2017. Protein-polysaccharide associative interactions in the design of tailor-made colloidal particles. Curr. Opin. Colloid Interface Sci. 28, 15–21. https://doi.org/10.1016/j.cocis.2016.12.003.
Seo, S., Karboune, S., L'Hocine, L., Yaylayan, V., 2013. Characterization of glycated lysozyme with galactose, galactooligosaccharides and galactan: effect of glycation on structural and functional properties of conjugates. LWT–Food Sci. Technol. 53 (1), 44–53. https://doi.org/10.1016/j.lwt.2013.02.001.
Seta, L., Baldino, N., Gabriele, D., Lupi, F.R., de Cindio, B., 2014. Rheology and adsorption behaviour of beta-casein and beta-lactoglobulin mixed layers at the sunflower oil/water interface. Colloids Surf. A Physicochem. Eng. Asp. 441, 669–677. https://doi.org/10.1016/j.colsurfa.2013.10.041.
Tian, T., Tong, X.H., Yuan, Y., Lyu, B., Jiang, D.Z., Cui, W.Y., Cheng, X.Y., Li, L., Li, Y., Jiang, L.Z., Wang, H., 2021. Preparation of benzyl isothiocyanate nanoemulsions by different emulsifiers: stability and bioavailability. Process Biochem. 111, 128–138. https://doi.org/10.1016/j.procbio.2021.09.001.
Tian, Y., Zhang, Z., Zhang, P.P., Taha, A., Hu, H., Pan, S.Y., 2020. The role of conformational state of pH-shifted beta-conglycinin on the oil/water interfacial properties and emulsifying capacities. Food Hydrocolloids 108, 105990. https://doi.org/10.1016/j.foodhyd.2020.105990.
Wang, S.N., Yang, J.J., Shao, G.Q., Qu, D.N., Zhao, H.K., Yang, L.N., Zhu, L.J., He, Y.T., Liu, H., Zhu, D.S., 2020a. Soy protein isolated-soy hull polysaccharides stabilized O/W emulsion: effect of polysaccharides concentration on the storage stability and interfacial rheological properties. Food Hydrocolloids 101, 105490. https://doi.org/10.1016/j.foodhyd.2019.105490.
Wang, W.D., Li, C., Zhang, B., Huang, Q., You, L.J., Chen, C., Fu, X., Liu, R.H., 2020b. Physicochemical properties and bioactivity of whey protein isolate-inulin conjugates obtained by Maillard reaction. Int. J. Biol. Macromol. 150, 326–335. https://doi.org/10.1016/j.ijbiomac.2020.02.086.
Xiong, W.F., Ren, C., Tian, M., Yang, X.J., Li, J., Li, B., 2018. Emulsion stability and dilatational viscoelasticity of ovalbumin/chitosan complexes at the oil-in-water interface. Food Chem. 252, 181–188. https://doi.org/10.1016/j.foodchem.2018.01.067.
Yao, X.L., Wang, N., Fang, Y.P., Phillips, G.O., Jiang, F.T., Hu, J.Z., Lu, J., Xu, Q., Tian, D., 2013. Impact of surfactants on the lipase digestibility of gum Arabic-stabilized O/W emulsions. Food Hydrocolloids 33 (2), 393–401. https://doi.org/10.1016/j.foodhyd.2013.04.013.
Yi, J., Li, Y., Zhong, F., Yokoyama, W., 2014. The physicochemical stability and in vitro bioaccessibility of beta-carotene in oil-in-water sodium caseinate emulsions. Food Hydrocolloids 35, 19–27. https://doi.org/10.1016/j.foodhyd.2013.07.025.
Yi, J., Zhong, F., Zhang, Y.Z., Yokoyama, W., Zhao, L.Q., 2015. Effects of lipids on in vitro release and cellular uptake of beta-carotene in nanoemulsion-based delivery systems. J. Agric. Food Chem. 63 (50), 10831–10837. https://doi.org/10.1021/acs.jafc.5b04789.
Zhang, G.R., Li, Y.H., Song, T.W., Bao, M.T., Li, Y.M., Li, X.M., 2019. Improvement in emulsifying properties of whey protein-rhamnolipid conjugates through short-time heat treatment. Colloids Surf. B Biointerfaces 181, 688–695. https://doi.org/10.1016/j.colsurfb.2019.06.015.
Zhong, L., Ma, N., Wu, Y.L., Zhao, L.Y., Ma, G.X., Pei, F., Hu, Q.H., 2019. Gastrointestinal fate and antioxidation of beta-carotene emulsion prepared by oat protein isolate-pleurotus ostreatus beta-glucan conjugate. Carbohydr. Polym. 221, 10–20. https://doi.org/10.1016/j.carbpol.2019.05.085.
Zhong, S.R., Li, M.F., Zhang, Z.H., Zong, M.H., Wu, X.L., Lou, W.Y., 2021. Novel antioxidative wall materials for lactobacillus casei microencapsulation via the maillard reaction between the soy protein isolate and prebiotic oligosaccharides. J. Agric. Food Chem. 69 (46), 13744–13753. https://doi.org/10.1021/acs.jafc.1c02907.